Critical Dynamics*

R. Folk
Institute for Theoretical Physics, University of Linz, Austria

April 7, 2003

Abstract

An introduction into the field of critical dynamics is given and recent progress made is presented. Comparison between experiments in fluids, ferromagnets and superfluid helium with field theoretical calculations is made.

1 Introduction

Critical phenomena are everyday life experiences, mostly we are confronted with first order phase transitions. However under certain circumstances we may observe second order phase transitions. An example is the the gas liquid critical point in a fluid. There we observe a spectacular behavior of physical quantities, most prominently examples are the diverging of the specific heat and the critical opalescence.

Historically the experimental study of second order phase transition behavior started in the midth of the 19th century. Theoretical explanations developed: Van der Waals theory for fluids, mean field theory for magnets and then more generally Landau theory. Already 1896 Verschaffelt recognized differences to the predictions of mean field theory in fluids. Later on Onsager solved the two dimensional Ising model proving the mean field theory to be inadequat to calculate e.g. the critical exponents.

Finally the critical behavior could be explained by renormalization group (RG) theory 1971, which also proved already developed concepts as universality for e.g. the exponents and amplitutde ratios in the power laws for the dependence of physical quantities. Moreover the concept of scaling naturally arises due to the diverging of the correlation length and the invariance with respect to RG transformations. RG

*Ising lecture held in Lviv April 2003. Draft version connects a specific critical behavior to the existence of a stable fixed point and the attraction of the 'flow' of model parameters to this fixed point.

More complicated and more realistic situations could be explained by the existence of additional fixed points and a crossover from unstabel fixed points to the stable fixed point. The knowledge in this field - static critical behavior - is collected already in several textbooks and I mention just a couple of them [1] (containig field theoretic methods).

Dynamical critical behavior was less understood but the phenomenon of critical slowing down (the characteristic time τ_c for dynamical phenomena diverges when one approaches the critical point) was recognized and Van Hove theory (1954) could give an explanation although it assumes that transport coefficients and/or kinetic coefficients remain uncritical. It was not understood how the diverging correlations of the static fluctuations affect the transport coefficients. In the sixties scaling ideas where applied to dynamical phenomena too and parallel to mode coupling theory dynamical scaling theory evolved into the formulation of dynamical renormalization group theory. This development up to 1977 is summarized in the review of Halperin Hohenberg [2].

Although dynamical phenomena are more complicated than static ones all the concepts know in statics can also be found in dynamics. These are: (i) universality (power laws with universal exponents and universal amplitude ratios in the asymptotics), (ii) scaling properties (in the asymptotics), (ii) crossover phenomena. In defining certain dynamical universality classes an important role however is played by the conservation properties of the order parameter (OP) and the dynamical coupling to other conserved densities. Thus models described by the same static functional may be in different dynamical universality classes.

2 Experimental evidence

In this section I collect some examples of dynamical critical behavior subject of *quantitative* theoretical calculations within dynamical renormalization group theory. It is a personal selection and mainly reflects own research in which I cooperated with others. The experimental result are in most cases the most recent ones presenting the state of art.

2.1 Fluids

In fluids two transport coefficents are of most interest the shear viscosity and the thermal conductivity. They are directly connected to the dynamical model describing the dynamical critical behavior. However there are other transport coefficients which show critical behavior but they are not the primary ones. An example is the sound mode, where the sound velocity and the sound absorption show critical behavior. Let first look at experimental results for the shear viscosity (see Fig. 1).

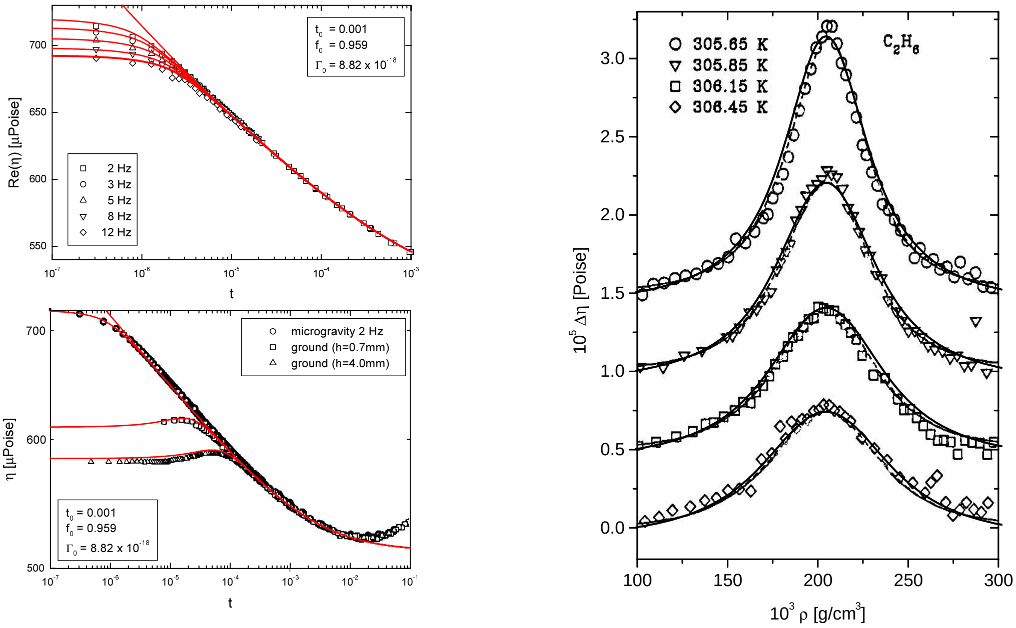

Figure 1: (a) Temperature dependence of the shear viscosity of Xenon with and without gravity for different frequencies. [3, 4] (b) Density dependence of the shear viscosity of C_2H_6 for different temperatures [5]. The curves were shifted for better clearness.

The temperature dependence has been measured on earth and in space (reduced gravity). On earth near the phase transition a finite value is reached. This is due to the earth's gravity which couples to the density. In the specific measurements of the shear viscosity with oscillating discs within cells of a certain height gravity produces a density distribution around the critical density in the midth of the cell. Thus one has to take into account that one is not at the critical density. This makes the shear viscosity at T_c finite (and the finite value depends on the height of the cell). Fig. 1(b) shows the shear viscosity as function of density around the critical density. A possible divergence of the shear viscosity with a power law may only be observed in reducing the gravitational effects e.g. by going to space. Experimental results are shown in the upper figure of Fig. 1(a). However the evolution of a power law is recognized but finally near T_c again a finite value is reached. The physical reason is the fact that the experiment is made at a small but finite frequency, which means again the experiment is not *at* criticality (criticality means: $T = T_c$ and $\rho = \rho_c$ or $\xi = \infty$, $k = 0$ and $\omega = 0$).

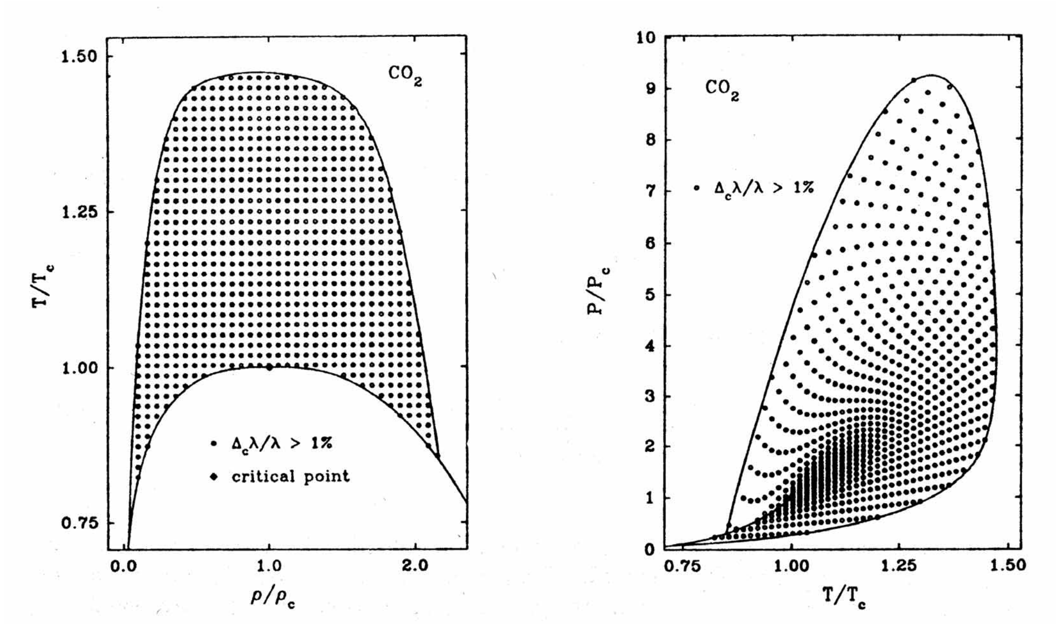

Figure 2: Region for CO_2 of more than 1% enhancement to the thermal conductivity due to fluctuations. Taken from [6].

Also the thermal conductivity is strongly enhanced when approaching the critical point and a power law divergence can be observed. The region where fluctuations contribute is shown in Fig. 2.

2.2 Ferromagnets

Neutron scattering is the main technique to study magnetic critical phenomena. However this is a little bit more complicated than what we have discussed so far since the dynamical susceptibility taken from theory has to be folded with a resolution function characteristic for the experimental setup. In this way one may look at the shape and the width of the scattering function (intensity) either in a experimental setup where the wave vector is kept constant during the measurement or the energy transfer is kept constant. Let us consider the shape of the scattering function at T_c. In Fig. 3 the intensity is compared with a Lorentzian and a non Lorentzian shape function. It is clearly demonstarted that the shape is non Lorentzian and this is attributed to dynamical fluctuation effects. At T_c the width at half height as function of wave vector shows a power law with an exponent of roughly 2.5

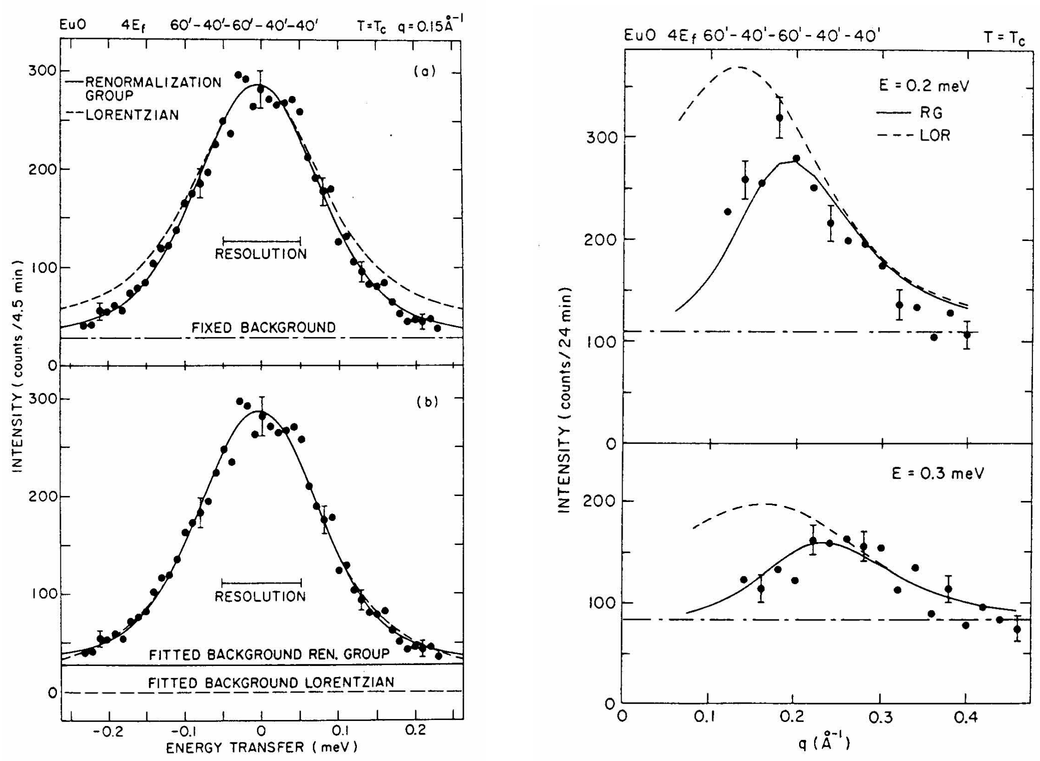

Figure 3: (a) Constant wave vector scans in EuO (b) Constant energy scans in EuO. Both demonstrate deviations from a Lorentzian shape function. [7]

2.3 Superfluid ^{4}He

The superfluid transition is an exeptional example of a second order phase transition since the symmetry breaking is exact (a second system is the antiferromagnet). No physical field is conjugate to the order parameter. It is also exceptional with respect to the existence of a whole line of phase transitions as function of pressure. This makes it an ideal system for testing universality.

The thermal transport properties are of main interest. This transport is diffusive above T_λ and propagating (second sound) below T_λ. We show the thermal conductivity λ for different pressures as function of temperature. A power law divergence seems to be observable, but looking closer to the data by extracting the universal amplitude R_λ^{exp}

$$R_\lambda^{exp} = \frac{\lambda}{g_0\sqrt{\xi C_p}} \tag{1}$$

involving the specific heat C_p, the correlation length ξ and a constant g_0. This amplitude is expected to go to a universal constant near T_λ, but turns out to be temperatur and pressure dependent even in the range of relative temperature dis-

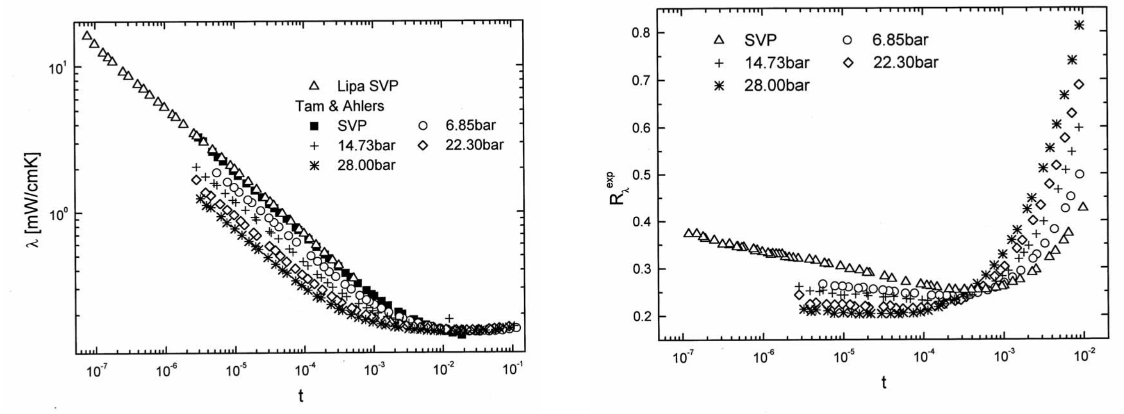

Figure 4: (a) Temperature dependence of the thermal conductivity of ^{4}He for different pressures near the superfluid transition. [8, 9] (b) The same for the amlitude ratio, which should be universal and was expected to be temperature and pressure independent.

tances as 10^{-6} and 10^{-7}. These remarkable data (see Fig. 4 at saturated vapor pressure have been obtained in a space shuttle mission. Even for the supefluid transition it is necessary to go to reduced gravity in order to get reliable data. In statics one comes to phantastic values of 10^{-9} to 10^{-10} (in specific heat measurements) for the relative temperature distances.

3 Van Hove theory

Let us consider a model described by the most simple dynamical equation, which might be suitable for a one component order parameter ψ_k (OP, non conserved or conserved). One may have in mind the magnetization then equation describes simply the relaxation (if non conserved) or diffusion (if conserved) mode present in this system

$$\frac{\partial \psi_k(t)}{\partial t} = -\Gamma k^a (r + k^2)\psi_k(t) + \zeta_k(t) \tag{2}$$

where $a = 0$ or $a = 2$ for a non conserved or a conserved OP respectively. The OP is a slow variable all other variables are assumed to be fast and represented in the dynamical equation by Gaussian distributed fluctuating forces. In order to reach in equilibrium the correct statics the Einstein relation

$$< \zeta_k(t)\zeta_{k'}(t') >= 2\Gamma k^a \delta_{k-k'}\delta(t - t') \tag{3}$$

has to be fulfilled. From this equation the dynamic susceptibility

$$< \psi(\vec{x}, t)\psi(\vec{x}', t') >_\zeta \;\; = \;\; \chi_{dyn}(\vec{x} - \vec{x}', t - t') \tag{4}$$

$$\chi_{dyn}(\vec{k},\omega) = <\psi(\vec{k},\omega)\psi(-\vec{k},-\omega)>_\zeta \tag{5}$$

$$\psi_{k,\omega} = \frac{\zeta_{k,\omega}}{-i\omega+\Gamma k^a(r+k^2)} \tag{6}$$

$$\chi_{dyn}(k,\omega) = \frac{2\Gamma k^a}{\omega^2+\{\Gamma k^a(r+k^2)\}^2} \tag{7}$$

is easily calculated. Integration over ω gives the static susceptibility

$$\chi_{st}(k,\xi) = \frac{1}{r+k^2} \qquad r=\xi^{-2} \tag{8}$$

A characteristic frequency may be defined by the halfwidth at half height

$$\omega_c(k,\xi) = \Gamma k^a(\xi^{-2}+k^2) \tag{9}$$

and with these definitions the result for the dynamic suscsptibility can be cast into scaling form

$$\chi_{dyn}(k,\omega,\xi) = \frac{\chi_{st}(k,\xi)}{\omega_c(k,\xi)} F\left(\frac{\omega}{\omega_c(k,\xi)}, k\xi\right) \tag{10}$$

definig the shape function F.

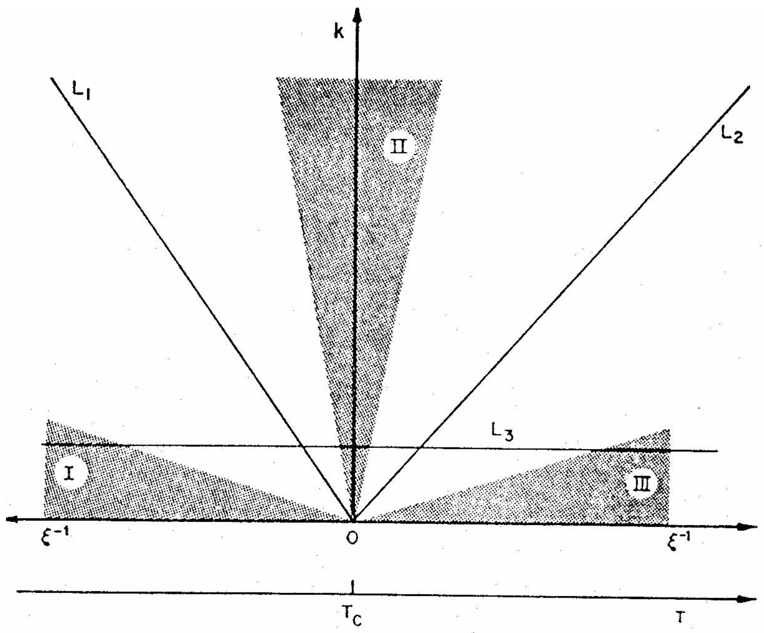

Figure 5: I: hydrodynamic region below T_c, II: critical region below and above T_c and III: hydrodynamic region above T_c

The characteristic frequency may be written in scaling form

$$\omega_c(k,\xi) = Ak^z\Omega(k\xi) \tag{11}$$

defining the dynamical critical exponent

$$z = 2 + a \tag{12}$$

and the scaling function

$$\Omega(x) = \left(\frac{1}{x^2} + 1\right) \tag{13}$$

This function has in the critical region and in the hydrodynamic region the limiting behavior

$$\omega_c = \begin{cases} Ak^z & k\xi >> 1 \\ Ak^{z-2}\xi^{-2} & k\xi << 1 \end{cases} \tag{14}$$

The shape function is given by a Lorentzian

$$F(y,x) = \frac{2}{y^2+1} \qquad y = \frac{\omega}{\omega_c} \tag{15}$$

and independent from x. That means the shape is the same in the critical and in the hydrodynamic region.

Although the Van Hove model [10] captures some features observed in experiments qualitatively (e.g. behavior of the characteristic frequency) it failes quantitatively. One also sees from the calculation that the behavior of the characteristic frequency is just a consequence of the critical behavior of the static susceptibility. No genuine 'dynamical' critical contribution is present.

4 Dynamical scaling

We now generalize by assuming that scaling holds but with general values for the exponts and the scaling functions [11]. In this way already an analysis of experiment can be performed and exponents and scaling functions can be extracted. This however relies on the assumption that the system has reached already the asymptotic region. As an example shown in Fig. 6 the linewidth of Xenon as function of temperature for different wave vectors. Introducing the scaling variables

$$\xi = \xi_o t^{-\nu} \qquad x_\eta \sim 0.04 \qquad x = k\xi \qquad \frac{\omega_c \xi^{1+x_\eta}}{k^2 \Gamma_{as}} = \Omega(x) \tag{16}$$

the data at different wave vector k of Fig. 6(a) collapse almost on one curve - the scaling function - shown in Fig. 6(b). However a warning should be expressed at this place because non-asymptotic effects may be less visible in such a scaling plot.

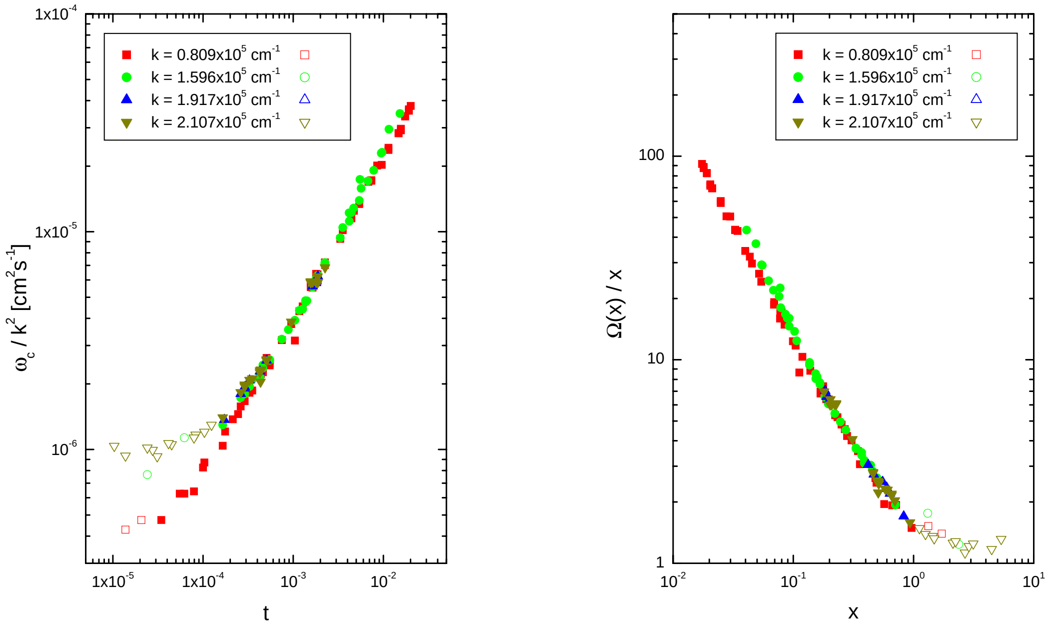

Figure 6: (a) Linewidth data of light scattering intensity in Xenon [12] (b) in scaled variables

4.1 Scaling form of the dynamic susceptibility

The scaling form of the dynamic susceptibility χ_{dyn} of the OP reads

$$\chi_{dyn}(\xi, k, \omega) = \frac{\chi_{st}(\xi, k)}{\omega_c(\xi, k)} F\left(\frac{\omega}{\omega_c(\xi, k)}, k\xi\right) \tag{17}$$

As well as the characteristic frequenzy ω_c (Eq. 13 width at half height) the static correlation function χ_{st}

$$\chi_{st}(\xi, k) = k^{-2+\eta} g(k\xi) \tag{18}$$

can be written in scaling form. This leads to the dynamic scaling function (masterfunktion) $F(y, x)$ ($y = \omega/\omega_c(\xi, k)$ and $x = k\xi$) which determines the shape. It fulfills since ω_c is the halfwidth at half height,

$$\int dy F(y, x) = 2\pi \quad \text{und} \quad F(1, x) = \frac{1}{2} F(0, x) \tag{19}$$

As a consequence of the validity of scaling one obtaines a change of the shape crossing over from the hydrodynamic region to the critical region.

In the hydrodynamic region $k\xi \ll 1$, the characteristic frequency is given by the hydrodynamic mode (we think of a conserved OP as for the case of a ferromagnet) $\omega_c = Dk^2$ and the static susceptibility reads $\chi \sim \xi^{\frac{\gamma}{\nu}}$. In consequence we find the temperature dependence of the diffusion coefficient

$$D(\xi) = \Gamma(\xi)/\chi_{st}(\xi, 0) \sim \xi^{2-z} \qquad \text{and} \qquad \Gamma(\xi) \sim \xi^{2-z+\frac{\gamma}{\nu}} \tag{20}$$

and the OP Onsager coefficient Γ. Note that in van Hove theory (statics described by mean field theory) one immedeately gets $z = 4$ since $\gamma/\nu = 2$ in order to have an uncritical transport coefficient. The shape function calculated within hydrodynamics has a Lorentzian shape

$$F(y, x << 1) = \frac{1}{y^2 + 1} \tag{21}$$

In the critical region, $k\xi \gg 1$ or $T = T_c$, the characteristic frequency and the static susceptibility are given by $\omega_c \sim k^z$ and $\chi \sim k^{-2+\eta}$ respectively and the dynamic susceptibility scales as

$$\chi_{dyn}(k, \omega) \sim k^{-z-2+\eta} F(y, \infty) \tag{22}$$

We now make use of the conservation property of the OP which demands for $k \to 0$ and $\omega \to 0$ that $\chi_{dyn} \sim k^2$. This leads to the following y dependence in the hydrodynamic and critical limit

$$\begin{aligned} F(y, \infty) &\sim \text{const.} \qquad \text{for} \qquad y \to 0 \\ F(y, \infty) &\sim y^{-\frac{z+4-\eta}{z}} \qquad \text{for} \qquad y \to \infty \end{aligned}$$

Thus for $z \neq 4$ and $\eta \neq 0$ one recognizes that the decay of the shape function for large scaling argument is non-Lorentzian. For a ferromagnet this would be ($z \sim 2.5$)

$$F \sim y^{-2.6} \qquad \text{instead of} \qquad F \sim y^{-2} \tag{23}$$

4.2 Finding the dynamical exponent z by scaling relations

4.2.1 Ferromagnet

Let us consider a ferromagnet below T_c. Due to the symmetry breaking of the continous symmetry (in OP-space) by the non zero OP a symmetry restoring propagating mode (Goldstane mode) is present - the spin wave mode. Is dispersion (undamped) in the hydrodynamic region is given by ($d = 3$)

$$\omega_c^- = vk^2 \qquad v \sim \frac{\rho_{stiff}}{M} \sim \xi^{-1+\beta/\nu} \tag{24}$$

The 'spin wave velocity' v is a static quantity and is expressed by the transverse correlation length and the magnetisation (OP). On the other hand it defines a characteristic frequency fulfilling dynamical scaling

$$\omega_c^- \sim k^z \Omega^-(k\xi) \sim \xi^{2-z} k^2 \tag{25}$$

Comparing with the dispersion

$$2 - z = -1 + \beta/\nu \qquad \to \qquad z = 3 - \beta/\nu = (5 - \eta)/2 \tag{26}$$

leads to the value of the dynamical exponent. Use has been made of static scaling laws $2\beta + \gamma = 2 - \alpha = 3\nu$ in $d = 3$ and $\gamma/\nu = 2 - \eta$ then $\beta/\nu + 1 - \eta/2 = 3/2$

Since z is now known we can make predictions on the temperature dependence of the spin diffusion constant in the hydrodynamic region above T_c

$$\omega_c^+ = Dk^2 \sim k^z \Omega^+(k\xi) \qquad D \sim \xi^{2-z} \sim \xi^{(-1+\eta)/2} \tag{27}$$

4.2.2 Fluids

In the liquid the thermal transport below and above is diffusive and nothing can be gained at the moment.

4.2.3 Superfluid transition

Similar to the ferromagnet also in superfluid ^{4}He below T_λ one has a propagating mode - the second sound mode, which is the corresponding Goldstone mode. Its dispersion reads (undamped) in the hydrodynamic region ($d = 3$)

$$\omega_c^- = vk \qquad v \sim \left(\frac{\rho_{stiff}}{c_p}\right)^{1/2} \sim \xi^{-1/2+\alpha/2\nu} \tag{28}$$

The second sound velocity v is a static quantity and is expressed by $\rho_{stiff} \sim \rho_s \sim$ and the specific heat $c_p \sim \xi^{\alpha/\nu}$. Comparing with the dynamical scaling law

$$\omega_c^- \sim k^z \Omega^-(k\xi) \sim \xi^{1-z} k \tag{29}$$

one finds again the critical dynamical exponent

$$1 - z = -1/2 + \alpha/2\nu \qquad \to \qquad z = 3/2 - \alpha/2\nu \tag{30}$$

Since α turns out to be smaller than but almost equal to zero one has in fact $z = 3/2$.

Since z is now known we can make predictions on the temperature dependence of the thermal diffusion constant in the hydrodynamic region above T_c

$$\omega_c^+ = Dk^2 \sim k^z \Omega(k\xi) \qquad D \sim \xi^{2-z} \sim \xi^{1/2+\alpha/2\nu} \tag{31}$$

Since at $n = 2$ the specific heat does not diverge α has in fact to be taken equal to 0. The superfluid transition is above but very near the borderline where the specific heat exponent changes sign so that an almost logarithmic temperature dependence in the specific heat is observed.

Tab. 4.2.3 summarizes the dynamical critical exponents for different systems

model	name	system	Goldstone mode	dyn. exp.
relaxation	A	FeF_2	-	$2 + c\eta \sim 2$
diffusion	B		-	$4 - \eta \sim 4$
relaxation	C		-	$2 + \alpha/\nu$ $(n = 1)$
relaxation	C		-	$2 + c\eta$ $(n \geq 2)$
symm. planar m.	E	XY Magnet	spin wave	3/2
asymm. planar m.	F	^4He	2. sound	3/2
antiferromagnet	G	$RbMgF_3$	spin wave	3/2
fluid	H	Xenon	-	$3 + x_\eta \sim 3$
ferromagnet	J	Fe	spin wave	$1/2(5 - \eta) \sim 5/2$

5 From dynamic equations to a Lagrangian

The steps to set up a model for the critical dynamics follow a systematic procedure. The time scale is set by the OP and the fact that one observes critical slowing down. Therefore one has to consider besides the OP (conserved or not) the slow densities in the system, which are the densities of the conserved quantities. Thus the set of densities to be consider is enlarged in comparison to statics. In a first step one has to reconsider the static functional including the additional densities.

In the second step one has to find out the equations of motion for these slow variables. The fast variables are included as stochastic forces in the equations of motion for the slow variables. The fast variables also related to damping effects. The form of the equations of motion are know in general and fulfill the following conditions: (i) the system reaches due to irreversible terms in the dynamic equations the statics described by the static functional derived in the first step, (ii) in the hydrodynamic limit the sytsem reproduces the known hydrodynamic equations leading to the reversibel terms given by Poisson brackets. In order to fulfill (i) the stochastic forces - Gaussian distributed - have to obey Einstein relations. The Poisson brackets may be derived using certain symmetry groups inherent in the given problem [20]. These symmetry group properties leading to the Poisson brackets are equivalent to the symmetries considered to derive Ward identities. They play an important role to find out the renormalization of the dynamic mode coupling and lead to the dynamic scaling relations expressing the dynamical exponent z already found by connecting the characteristic frequency above and below T_c in systems with a propagating mode in the condensed phase.

In the following I recapitulate the appendices of Ref. [13].

5.1 Static Functional

I will sketch only briefly the derivation of a static functional for pure liquids. The starting point is a local equilibrium distribution function

$$w_{loc} = \frac{1}{\mathcal{N}} e^{-\int_V d^d x \frac{\Omega(x)}{k_B T(x)}} \tag{32}$$

with temperature $T(x)$, chemical potential $\mu(x)$ and velocity $\boldsymbol{v}(x)$ as external fields. $\Omega(x)$ is the corresponding local thermodynamic potential

$$\Omega(x) = e(x) + e_k(x) - T(x)s(x) - \mu(x)\rho(x) - \boldsymbol{v}(x)\boldsymbol{j'}(x) \tag{33}$$

in which $e(x)$ is the internal energy density and $e_k(x) = \boldsymbol{j'}(x)^2/2\rho(x)$ is the kinetic energy density. Assuming that the densities are fluctuating about their thermodynamic average values, we can write

$$\begin{aligned} e(x) &= e + \triangle e(x) \ , \qquad e_k(x) = e_k + \triangle e_k(x) \ , \\ s(x) &= s + \triangle s(x) \ , \qquad \rho(x) = \rho + \triangle\rho(x) \ , \\ \boldsymbol{j'}(x) &= \boldsymbol{j'} + \triangle\boldsymbol{j'}(x) \ . \end{aligned} \tag{34}$$

Additionally we allow small variations of the conjugated external fields.

$$\begin{aligned} T(x) &= T + \delta T(x) \ , \qquad \mu(x) = \mu + \delta\mu(x) \ , \\ \boldsymbol{v}(x) &= \boldsymbol{v} + \delta\boldsymbol{v}(x) \ . \end{aligned} \tag{35}$$

Inserting (34) and (35) in (33) the local thermodynamic potential can be splitted into three parts

$$\frac{\Omega(x)}{k_B T} = \frac{\Omega^{(0)}}{k_B T} + \mathcal{H}(x) - \delta\mathcal{H}(x) \ . \tag{36}$$

The first part represents the thermodynamic average and contains the Gibb's free energy $\Omega^{(0)} = e + e_k - Ts - \mu\rho - \boldsymbol{v}\boldsymbol{j'}$. The second part involves the fluctuation contributions and is given by

$$\mathcal{H}(x) = \frac{1}{k_B T}(\triangle e(x) + \triangle e_k(x) - T \triangle s(x) - \mu \triangle \rho(x) - \boldsymbol{v} \triangle \boldsymbol{j'}(x)) \ . \tag{37}$$

The third part are the first order contributions due to the external field variation.

$$\begin{aligned} \delta\mathcal{H}(x) &= \frac{e(x) + e_k(x) - \mu\rho(x) - \boldsymbol{v}\boldsymbol{j'}(x)}{k_B T} \frac{\delta T(x)}{T} \\ &+ \frac{\rho(x)\delta\mu(x)}{k_B T} + \frac{\boldsymbol{j'}(x)\delta\boldsymbol{v}(x)}{k_B T} \ . \end{aligned} \tag{38}$$

Inserting (36) into the local distribution function (32) and expanding in first order of the external field variations, we get analogous to [14] for the correlation functions.

$$\langle s\ s\rangle_c = k_B T \left(\frac{\partial s}{\partial T}\right)_\mu \ , \qquad \langle \rho\ \rho\rangle_c = k_B T \left(\frac{\partial \rho}{\partial \mu}\right)_T \ , \tag{39}$$

$$\langle s\ \rho\rangle_c = k_B T \left(\frac{\partial\rho}{\partial T}\right)_\mu = k_B T \left(\frac{\partial s}{\partial\mu}\right)_T \ . \tag{40}$$

From (39) and (40) one can see that the thermodynamic derivatives involve the chemical potential μ. Experimentally the pressure P is accessible and therefore for a comparison with experimental measured quantities the local thermodynamic potential (36) has to be expressed in densities, which correspond to external fields T and P instead of T and μ. This can be obtained by changing from entropy density per volume $s(x)$ to entropy density per mass $\sigma(x) = s(x)/\rho(x)$. The corresponding fluctuations transform like

$$\triangle s(x) = \rho \triangle \sigma(x) + \sigma \triangle \rho(x) \ . \tag{41}$$

The correlation functions (39) and (40) change to

$$\langle\sigma\ \sigma\rangle_c = \frac{k_B T}{\rho}\left(\frac{\partial\sigma}{\partial T}\right)_P \ , \qquad \langle\rho\ \rho\rangle_c = \rho k_B T \left(\frac{\partial\rho}{\partial P}\right)_T \ , \tag{42}$$

$$\langle\sigma\ \rho\rangle_c = \frac{k_B T}{\rho}\left(\frac{\partial\rho}{\partial T}\right)_P = \rho k_B T \left(\frac{\partial\sigma}{\partial P}\right)_T \ . \tag{43}$$

Expanding the Hamiltonian (37) in powers of the fluctuations of the entropy per mass, the mass density and the momentum density we get

$$\begin{aligned} H \ &= \ \int d^d x \ \Big\{ \frac{1}{2} a_{\sigma\sigma}(\triangle\sigma(x))^2 + \frac{1}{2} c_{\sigma\sigma}(\boldsymbol{\nabla} \triangle \sigma(x))^2 + \frac{1}{2} a_{\rho\rho}(\triangle\rho(x))^2 \\ &+ \ a_{\sigma\rho} \triangle \sigma(x) \triangle \rho(x) + + \frac{1}{2} a'_j (\triangle \boldsymbol{j'}(x))^2 \\ &+ \ \frac{1}{3!} v_\sigma (\triangle\sigma(x))^3 + \frac{1}{4!} u_\sigma (\triangle\sigma(x))^4 + \frac{1}{2}\gamma_\rho \triangle \rho(x)(\triangle\sigma(x))^2 \Big\} \ . \end{aligned} \tag{44}$$

For dynamic calculations it is convenient to choose the entropy density fluctuations as order parameter. With regard to this we have expanded in (44) the entropy density fluctuations up to fourth order, while the mass density and momentum density fluctuations, considered as secondary densities, only need to be expanded up to quadratic order, taking into account in the Hamiltonian all terms relevant for the critical theory. The Gaussian part of (44) is non-diagonal and contains terms which are not invariant against order parameter inversion. These terms proportional to $\triangle\rho \triangle \sigma$ and $(\triangle\sigma)^3$ can be removed by introducing a shifted order parameter $\phi_0(x)$ and a transformed secondary density $q_0(x)$ like

$$\phi_0(x) \ = \ \sqrt{N_A}(\triangle\sigma(x) - \langle\triangle\sigma(x)\rangle) \ , \tag{45}$$

$$q_0(x) \ = \ \sqrt{N_A}\left[\triangle\rho(x) - \left(\frac{\partial\rho}{\partial\sigma}\right)_P (\triangle\sigma(x) - \langle\triangle\sigma(x)\rangle)\right] \ . \tag{46}$$

N_A has been introduced for convenience to obtain the appearance of the gas constant R instead of the Boltzmann constant k_B in the equations and parameter definitions. Introducing a rescaled momentum density $\boldsymbol{j} = \boldsymbol{j}_l + \boldsymbol{j}_t = \sqrt{N_A} \triangle \boldsymbol{j}'$, one ends up with the final expression for the static functional

$$\begin{aligned} H \ &= \ \int d^d x \ \Big\{ \frac{1}{2} \overset{o}{\tau} \phi_0^2(x) + \frac{1}{2}(\boldsymbol{\nabla}\phi_0(x))^2 + \frac{\overset{o}{\tilde{u}}}{4!}\phi_0^4(x) \\ &+ \ \frac{1}{2} a_q q_0^2(x) + \frac{1}{2} \overset{o}{\gamma}_q q_0(x)\phi_0^2(x) + \frac{1}{2} a_j \boldsymbol{j}_t^2(x) + \frac{1}{2} a_j \boldsymbol{j}_l^2(x) - \overset{o}{h}_q q_0(x) \Big\} \ , \end{aligned} \tag{47}$$

5.2 Dynamic Equations

Due to the critical slowing down the dynamics of critical phenomena is explicitly influenced mainly by slow processes. The influence of variables which vary on short time scales may be considered stochastically. Thus only projections of the dynamic variables into a subspace of slowly varying variables need to be considered [15, 16]. Let $\psi_i(x,t)$ be a set of slow variables, then the corresponding dynamic equations can be written as [17, 18, 19].

$$\frac{\delta\psi_i(x,t)}{\delta t} = V_i\{\psi(x,t)\} - \sum_j \Lambda_{ij}(x)\frac{\delta H\{\psi(x,t)\}}{\delta\psi_j(x,t)} + \Theta_i(x,t) \tag{48}$$

$\Theta_i(x,t)$ are fluctuating forces which fulfill the Einstein relations

$$\langle\Theta_i(x,t)\ \Theta_j(x',t')\rangle = 2\Lambda_{ij}(x)\delta(t-t')\delta(x-x') \tag{49}$$

when Markovian processes are assumed. $\Lambda_{ij}(x)$ are the kinetic coefficients, which are constants $\Lambda_{ij}(x) = \Lambda_{ij}$ in the case of non conserved densities $\psi(x,t)$ and are given by $\Lambda_{ij}(x) = -\Lambda_{ij}\nabla^2$ in the case of conserved densities. The reversible contributions $V_i\{\psi(x,t)\}$ of the dynamic equations can be written as[1]

$$V_i\{\psi(x,t)\} = \sum_j \int dx'dt' \left[\frac{\delta Q_{ij}(x,t;x',t')}{\delta\psi_j(x',t')} - Q_{ij}(x,t;x',t')\frac{\delta H\{\psi(x,t)\}}{\delta\psi_j(x',t')}\right] . \tag{50}$$

The quantities $Q_{ij}(x,t;x',t')$ are related to the Poisson brackets of the densities.

$$Q_{ij}(x,t;x',t') = k_BT\{\psi_i(x,t),\psi_j(x',t')\} . \tag{51}$$

For simple liquids the slowly varying densities $\psi_i(x)$ correspond to the volume densities $s(x), \rho(x)$ and $\boldsymbol{j'}(x)$. Generalized Poisson brackets for hydrodynamic densities may be derived from infinitesimal displacements [20]. The resulting Poisson brackets are

$$\begin{aligned} \{\boldsymbol{j'}(x,t), s(x',t')\} &= s(x,t)\boldsymbol{\nabla}\delta(x-x')\delta(t-t') , \\ \{\boldsymbol{j'}(x,t), \rho(x',t')\} &= \rho(x,t)\boldsymbol{\nabla}\delta(x-x')\delta(t-t') , \\ \{j'_k(x,t), j'_l(x',t')\} &= [j'_l(x,t)\nabla_k\delta(x-x') - j'_k(x',t')\nabla_l\delta(x-x')]\delta(t-t') . \end{aligned} \tag{52}$$

All other Poisson brackets are zero. The reversible terms (50) of the dynamic equations turn with (52) to (we omit the explicit indication of space and time dependence in the following)

$$V_s = -k_BT\boldsymbol{\nabla}\left(s\frac{\delta H}{\delta\boldsymbol{j'}}\right) , \tag{53}$$

$$V_\rho = -k_BT\boldsymbol{\nabla}\left(\rho\frac{\delta H}{\delta\boldsymbol{j'}}\right) , \tag{54}$$

$$\begin{aligned} \boldsymbol{V}_j &= -k_BT\left[s\boldsymbol{\nabla}\frac{\delta H}{\delta s} + \rho\boldsymbol{\nabla}\frac{\delta H}{\delta\rho}\right] \\ &\quad -k_BT\sum_k\left[j'_k\boldsymbol{\nabla}\frac{\delta H}{\delta j'_k} - \nabla_k\boldsymbol{j'}\frac{\delta H}{\delta j'_k}\right] . \end{aligned} \tag{55}$$

[1]The presence of reversible terms lead to organized motion. One of the simlest examples to imagine is the harmonic oscillator without damping, where the time derivative of the elongation couples to the momentum and the time derivative of the momentum to the elongation. This leads to an oscillatory motion. Similarly in magnets the reversible coupling leads to the Larmor precession below T_c, in liquids to sound waves, in superfluid He (below T_λ) to second sound.

The matrix Λ_{ij} is determined by the dissipation processes in hydrodynamics. For a liquid at rest ($\boldsymbol{v} = 0$) the hydrodynamic equation for the entropy density reads

$$T\frac{\partial s}{\partial t} = -\boldsymbol{\nabla}\boldsymbol{q} \ , \qquad \boldsymbol{q} = -\kappa_T^{(0)}\boldsymbol{\nabla}T \tag{56}$$

in which $\kappa_T^{(0)}$ is the thermal conductivity in the background. Expanding the functional H in (37) in powers of the fluctuations $\triangle s(x), \triangle\rho(x)$ and $\triangle\boldsymbol{j'}(x)$, a comparison of the coefficients in quadratic order with thermodynamic relations show that we can write $\nabla^2 T = k_B T\delta H/\delta s$. Thus the hydrodynamic equation (56) can be written as

$$\frac{\partial s}{\partial t} = k_B\kappa_T^{(0)}\nabla^2\frac{\delta H}{\delta s} \ . \tag{57}$$

From the above equation it follows that in the dynamic equation (48) for the entropy density the only non vanishing kinetic coefficient is $\Lambda_{ss} = -k_B\kappa_T^{(0)}\nabla^2$. With (53) we get

$$\frac{\partial s}{\partial t} = k_B\kappa_T^{(0)}\nabla^2\frac{\delta H}{\delta s} - k_B T\boldsymbol{\nabla}\left(s\ \frac{\delta H}{\delta\boldsymbol{j'}}\right) + \Theta_s \tag{58}$$

for the non linear entropy density equation. Due to mass conservation no dissipative contributions appear in the dynamic equation for the mass density. With (54) we simply get

$$\frac{\partial\rho}{\partial t} = -k_B T\boldsymbol{\nabla}\left(\rho\ \frac{\delta H}{\delta\boldsymbol{j'}}\right) \ . \tag{59}$$

The conservation of mass is an exact relation, therefore Eq.(59) contains no stochastic force. Linearizing the hydrodynamic equation for the momentum density in the velocity, the equation reads

$$\frac{\partial\boldsymbol{j'}}{\partial t} = (\zeta^{(0)} + \frac{\bar\eta^{(0)}}{3})\boldsymbol{\nabla}(\boldsymbol{\nabla}\boldsymbol{v}) + \bar\eta^{(0)}\nabla^2\boldsymbol{v} \tag{60}$$

$\zeta^{(0)}$ and $\bar\eta^{(0)}$ are the bulk viscosity and the shear viscosity in the noncritical background. Eq.(60) may be separated in an equation for the longitudinal and transverse part of the momentum density according to $\boldsymbol{j'} = \boldsymbol{j'}_l + \boldsymbol{j'}_t$ with $\boldsymbol{\nabla}\times\boldsymbol{j'}_l = 0$ and $\boldsymbol{\nabla}\boldsymbol{j'}_t = 0$

$$\frac{\partial\boldsymbol{j'}_l}{\partial t} = (\zeta^{(0)} + \frac{4}{3}\bar\eta^{(0)})\nabla^2\boldsymbol{v}_l \ , \qquad \frac{\partial\boldsymbol{j'}_t}{\partial t} = \bar\eta^{(0)}\nabla^2\boldsymbol{v}_t \ . \tag{61}$$

From the kinetic energy in the static functional (37) it follows that the longitudinal and transverse velocity in (61) can be written as $\boldsymbol{v}_i = k_B T\delta H/\delta\boldsymbol{j'}_i$ $(i = l, t)$. With the reversible term (55) we get for the nonlinear dynamic equation

$$\begin{aligned}\frac{\partial\boldsymbol{j'}}{\partial t} &= k_B T(\zeta^{(0)} + \frac{4}{3}\bar\eta^{(0)})\nabla^2\frac{\delta H}{\delta\boldsymbol{j'}_l} + k_B T\bar\eta^{(0)}\nabla^2\frac{\delta H}{\delta\boldsymbol{j'}_t} \\ &- k_B T\left[s\ \boldsymbol{\nabla}\frac{\delta H}{\delta s} + \rho\ \boldsymbol{\nabla}\frac{\delta H}{\delta\rho}\right] \\ &- k_B T\sum_k\left[j'_k\boldsymbol{\nabla}\frac{\delta H}{\delta j'_k} - \nabla_k\boldsymbol{j'}\frac{\delta H}{\delta j'_k}\right] + \boldsymbol{\Theta}_{j'} \ .\end{aligned} \tag{62}$$

Changing from entropy per volume to entropy per mass $\sigma(x) = s(x)/\rho(x)$, analogous to statics, Eq.(58) turns into

$$\frac{\partial\sigma}{\partial t} = \frac{k_B\kappa_T^{(0)}}{\rho^2}\nabla^2\frac{\delta H}{\delta\sigma} - k_B T(\boldsymbol{\nabla}\sigma)\ \frac{\delta H}{\delta\boldsymbol{j'}} + \Theta_\sigma \ . \tag{63}$$

From (62) we get the corresponding equation for the momentum density

$$\begin{aligned}
\frac{\partial \boldsymbol{j'}}{\partial t} &= k_B T(\zeta^{(0)} + \frac{4}{3}\bar{\eta}^{(0)})\nabla^2 \frac{\delta H}{\delta \boldsymbol{j'}_l} + k_B T \bar{\eta}^{(0)} \nabla^2 \frac{\delta H}{\delta \boldsymbol{j'}_t} \\
&- k_B T \left[\rho\, \boldsymbol{\nabla} \frac{\delta H}{\delta \rho} - (\boldsymbol{\nabla}\sigma) \frac{\delta H}{\delta \sigma} \right] \\
&- k_B T \sum_k \left[j'_k \boldsymbol{\nabla} \frac{\delta H}{\delta j'_k} - \nabla_k \boldsymbol{j'} \frac{\delta H}{\delta j'_k} \right] + \boldsymbol{\Theta}_{j'} \ . \qquad (64)
\end{aligned}$$

The equation for the mass density (59) remains unchanged. Eqs.(59), (63) and (64) constitute a set of nonlinear equations which describe the dynamics of fluctuations in liquids. The equations

$$\frac{\partial \phi_0}{\partial t} = \overset{o}{\Gamma}\, \nabla^2 \frac{\delta H}{\delta \phi_0} + \overset{o}{L}_\phi\, \nabla^2 \frac{\delta H}{\delta q_0} - \overset{o}{g}\, (\boldsymbol{\nabla}\phi_0)\, \frac{\delta H}{\delta \boldsymbol{j}} + \Theta_\phi \ , \qquad (65)$$

$$\begin{aligned}
\frac{\partial q_0}{\partial t} &= \overset{o}{L}_\phi\, \nabla^2 \frac{\delta H}{\delta \phi_0} + \overset{o}{\lambda}\, \nabla^2 \frac{\delta H}{\delta q_0} - \overset{o}{c}\, \boldsymbol{\nabla} \frac{\delta H}{\delta \boldsymbol{j}_l} - \overset{o}{g}\, \boldsymbol{\nabla} \left(q_0 \frac{\delta H}{\delta \boldsymbol{j}} \right) \\
&- \overset{o}{g}_l\, \phi_0 \boldsymbol{\nabla} \frac{\delta H}{\delta \boldsymbol{j}_l} + \Theta_q \ , \qquad (66)
\end{aligned}$$

$$\begin{aligned}
\frac{\partial \boldsymbol{j}_l}{\partial t} &= \overset{o}{\lambda}_l\, \nabla^2 \frac{\delta H}{\delta \boldsymbol{j}_l} - \overset{o}{c}\, \boldsymbol{\nabla} \frac{\delta H}{\delta q_0} - \overset{o}{g}_l\, \boldsymbol{\nabla} \left(\phi_0 \frac{\delta H}{\delta q_0} \right) \\
&+ \overset{o}{g}\, (1 - \mathcal{T}) \left\{ (\boldsymbol{\nabla}\phi_0) \frac{\delta H}{\delta \phi_0} + q_0 \boldsymbol{\nabla} \frac{\delta H}{\delta q_0} \right\} \\
&- \overset{o}{g}\, (1 - \mathcal{T}) \left\{ \sum_k \left[j_k \boldsymbol{\nabla} \frac{\delta H}{\delta j_k} - \nabla_k \boldsymbol{j} \frac{\delta H}{\delta j_k} \right] \right\} + \boldsymbol{\Theta}_l \ , \qquad (67)
\end{aligned}$$

$$\begin{aligned}
\frac{\partial \boldsymbol{j}_t}{\partial t} &= \overset{o}{\lambda}_t\, \nabla^2 \frac{\delta H}{\delta \boldsymbol{j}_t} + \overset{o}{g}\, \mathcal{T} \left\{ (\boldsymbol{\nabla}\phi_0) \frac{\delta H}{\delta \phi_0} + q_0 \boldsymbol{\nabla} \frac{\delta H}{\delta q_0} \right\} \\
&- \overset{o}{g}\, \mathcal{T} \left\{ \sum_k \left[j_k \boldsymbol{\nabla} \frac{\delta H}{\delta j_k} - \nabla_k \boldsymbol{j} \frac{\delta H}{\delta j_k} \right] \right\} + \boldsymbol{\Theta}_t \ . \qquad (68)
\end{aligned}$$

are obtained by introducing the fields ϕ_0 and q_0 from (45) and (46) and by splitting the momentum density equation into a longitudinal and transverse part.

5.3 Dynamic Functional

In order to calculate the dynamic correlation functions in a perturbation expansion we need a generating dynamic functional. Considering the dynamic equations (65) to (68), we write the equations which contain stochastic forces in a short notation

$$\partial_t \vec{\alpha} = \vec{V} + \vec{\Theta} \qquad \text{with} \quad \vec{\alpha} = \begin{pmatrix} \sigma \\ \boldsymbol{j}'_l \\ \boldsymbol{j}'_t \end{pmatrix} \ , \quad \vec{\Theta} = \begin{pmatrix} \Theta_\sigma \\ \boldsymbol{\Theta}'_l \\ \boldsymbol{\Theta}'_t \end{pmatrix} \ . \qquad (69)$$

The vector $\vec{V}$ contains the rest of Eqs.(63) and (64). The fluctuating forces $\vec{\Theta}$ fulfill Einstein relations (Gaussian distributed stochastic force with correlation given by the coefficient matrix

$$\boldsymbol{L'} = \begin{pmatrix} -(k_B \kappa_T^{(0)}/\rho^2)\nabla^2 & 0 & 0 \\ 0 & -k_B T(\zeta^{(0)} + \frac{4}{3}\bar{\eta}^{(0)})\nabla^2 & 0 \\ 0 & 0 & -k_B T \bar{\eta}^{(0)} \nabla^2 \end{pmatrix} \ . \qquad (70)$$

Additionally we have the exact continuity equation (59) in the short form

$$\partial_t \rho = V_\rho \tag{71}$$

which may be considered as a constraint for the generating functional. The stochastic forces fluctuate in such a way that (71) always is fulfilled. Thus the generating functional (Onsager-Machlup functional) can be written as

$$Z_d = \int \mathcal{D}(\vec{\Theta})\ \mathcal{D}(F)\ \delta(F)\ \exp\left[-\frac{1}{4}\int dt\ dx\ \vec{\Theta}^T \boldsymbol{L}'^{-1}\vec{\Theta}\right] \tag{72}$$

where $F = \partial_t\rho - V_\rho$. $\mathcal{D}$ refers to a suitable integration measure. Inserting (69) and changing the integration variables leads to

$$\begin{aligned} Z_d &= \int \mathcal{D}(\vec{\alpha},\rho)\ \delta(\partial_t\rho - V_\rho) \\ &\times\ \exp\Big[-\frac{1}{4}\int dt\int dx\Big([\partial_t\vec{\alpha}-\vec{V}]^T\boldsymbol{L}'^{-1}[\partial_t\vec{\alpha}-\vec{V}] + 2\sum_i\frac{\delta V_i}{\delta\alpha_i} + 2\frac{\delta V_\rho}{\delta\rho}\Big)\Big]\ . \end{aligned} \tag{73}$$

The Delta function may be expressed by an exponential function

$$\delta(\partial_t\rho - V_\rho) = \int \mathcal{D}(i\tilde{\rho})\exp\Big[-\int dx\int dt\ \tilde{\rho}(\partial_t\rho - V_\rho)\Big]\ . \tag{74}$$

Introducing auxiliary fields $i\tilde{\vec{\alpha}}$ and performing a Gaussian transformation (73) turns into

$$Z_d = \int \mathcal{D}(\vec{\alpha},\rho,i\tilde{\vec{\alpha}},i\tilde{\rho})e^{-J} \tag{75}$$

with the Janssen-DeDominicis functional

$$J = \int dt\int dx\left(-\tilde{\vec{\alpha}}^T\boldsymbol{L}'\tilde{\vec{\alpha}} + \tilde{\vec{\alpha}}^T(\partial_t\vec{\alpha}-\vec{V}) + \tilde{\rho}(\partial_t\rho - V_\rho) + \frac{1}{2}\sum_i\frac{\delta V_i}{\delta\alpha_i} + \frac{1}{2}\frac{\delta V_\rho}{\delta\rho}\right)\ . \tag{76}$$

Introducing the order parameter (45) and the secondary density (46) in (76) the dynamic functional reads

$$J = \int dt\int dx\left(-\tilde{\vec{\beta}}^T\boldsymbol{L}\tilde{\vec{\beta}} + \tilde{\vec{\beta}}^T(\partial_t\vec{\beta}-\vec{V}) + \frac{1}{2}\sum_i\frac{\delta V_i}{\delta\beta_i}\right) \tag{77}$$

where the densities are $\vec{\beta}^T = (\phi_0, q_0, \boldsymbol{j}_l, \boldsymbol{j}_t)$ and $\boldsymbol{L}$ is the coefficient matrix

$$[L_{ij}] = \begin{pmatrix} -\overset{o}{\Gamma}\,\nabla^2 & -\overset{o}{L}_\phi\,\nabla^2 & 0 & 0 \\ -\overset{o}{L}_\phi\,\nabla^2 & -\overset{o}{\lambda}\,\nabla^2 & 0 & 0 \\ 0 & 0 & -\overset{o}{\lambda}_l\,\nabla^2 & 0 \\ 0 & 0 & 0 & -\overset{o}{\lambda}_t\,\nabla^2 \end{pmatrix}\ . \tag{78}$$

The conjugated densities $\tilde{\vec{\beta}}$ are defined accordingly. An explicit expression for (77) is obtained by inserting the dynamic equations (65)-(68). The Fourier transformed Gaussian part can be written as

$$J^{(0)} = \frac{1}{2}\int_{k,\omega}(\vec{\beta}^T(k,\omega),\tilde{\vec{\beta}}^T(k,\omega))\boldsymbol{\Gamma}^{(0)}(k,\omega)\begin{pmatrix}\vec{\beta}(-k,-\omega)\\ \tilde{\vec{\beta}}(-k,-\omega)\end{pmatrix}\ . \tag{79}$$

The integration is defined as $\int_{k,\omega} = \int\frac{d^dk}{(2\pi)^d}\ \int\frac{d\omega}{2\pi}$. The elements of the matrix $\boldsymbol{\Gamma}^{(0)}(k,\omega)$ are the dynamic vertex functions in lowest order perturbation theory. They are explicitly given by

$$\boldsymbol{\Gamma}^{(0)}(k,\omega) = \begin{pmatrix} \boldsymbol{0} & -i\omega\boldsymbol{1} + \boldsymbol{L}(k) \\ i\omega\boldsymbol{1} + \boldsymbol{L}^\dagger(k) & -2\boldsymbol{\lambda}(k)\end{pmatrix} \tag{80}$$

where $\mathbf{1}$ denotes the unit matrix and the superscript † the adjoint matrix. In the present case the submatrices are

$$\boldsymbol{L}(k) = \begin{pmatrix} \overset{o}{\Gamma}\, k^2(\overset{o}{\tau} + k^2) & \overset{o}{L}_\phi\, k^2(\overset{o}{\tau} + k^2) & -ik\, \overset{o}{g}_l \overset{o}{h}_q & 0 \\ a_q\, \overset{o}{L}_\phi\, k^2 & a_q\, \overset{o}{\lambda}\, k^2 & ika_q\, \overset{o}{c} & 0 \\ 0 & ika_j\, \overset{o}{c} & a_j\, \overset{o}{\lambda}_l\, k^2 & 0 \\ 0 & 0 & 0 & a_j\, \overset{o}{\lambda}_t\, k^2 \end{pmatrix} , \tag{81}$$

$$\boldsymbol{\lambda}(k) = \begin{pmatrix} \overset{o}{\Gamma}\, k^2 & \overset{o}{L}_\phi\, k^2 & 0 & 0 \\ \overset{o}{L}_\phi\, k^2 & \overset{o}{\lambda}\, k^2 & 0 & 0 \\ 0 & 0 & \overset{o}{\lambda}_l\, k^2 & 0 \\ 0 & 0 & 0 & \overset{o}{\lambda}_t\, k^2 \end{pmatrix} . \tag{82}$$

The interaction terms in the Hamiltonian (47) and the mode coupling terms in the dynamic equation modify the matrix (80) and may be calculated in a perturbation expansion. The dynamic two point vertex function are given by

$$\boldsymbol{\Gamma}(k,\omega) = \boldsymbol{\Gamma}^{(0)}(k,\omega) - \boldsymbol{\Sigma}(k,\omega) \tag{83}$$

where $\boldsymbol{\Sigma}(k,\omega)$ contains 1-irreducible diagrams with two external legs. The matrix $\boldsymbol{\Gamma}(k,\omega)$ of the vertex functions has the structure

$$\boldsymbol{\Gamma}(k,\omega) = \begin{pmatrix} [0] & [\Gamma_{\alpha,\tilde{\beta}}](k,\omega) \\ [\Gamma_{\tilde{\alpha},\beta}](k,\omega) & [\Gamma_{\tilde{\alpha},\tilde{\beta}}](k,\omega) \end{pmatrix} \tag{84}$$

with the submatrix

$$[\Gamma_{\alpha\tilde{\beta}}] = \begin{pmatrix} \overset{o}{\Gamma}_{\phi\tilde{\phi}} & \overset{o}{\Gamma}_{\phi\tilde{q}} & \overset{o}{\Gamma}_{\phi\tilde{l}} & 0 \\ \overset{o}{\Gamma}_{q\tilde{\phi}} & \overset{o}{\Gamma}_{q\tilde{q}} & \overset{o}{\Gamma}_{q\tilde{l}} & 0 \\ \overset{o}{\Gamma}_{l\tilde{\phi}} & \overset{o}{\Gamma}_{l\tilde{q}} & \overset{o}{\Gamma}_{q\tilde{l}} & 0 \\ 0 & 0 & 0 & \overset{o}{\Gamma}_{t\tilde{t}} \end{pmatrix} . \tag{85}$$

The submatrices $[\Gamma_{\tilde{\alpha},\beta}]$ and $[\Gamma_{\tilde{\alpha},\tilde{\beta}}]$ are defined accordingly. Then the propagators of the model are determined by inverting (80). In the limit $\overset{o}{c} \to \infty$ the propagators of order $(\overset{o}{c})^0$ are identical the known model H propagators. One gets the response propagators

$$\langle \phi_0(k,\omega)\ \tilde{\phi}_0(-k,-\omega)\rangle_0 = \frac{1}{-i\omega + \overset{o}{\Gamma}\, k^2(\overset{o}{\tau} + k^2)} , \tag{86}$$

$$\langle \boldsymbol{j}_t(k,\omega) \otimes \tilde{\boldsymbol{j}}_t(-k,-\omega)\rangle_0 = \frac{1}{-i\omega + a_j\, \overset{o}{\lambda}_t\, k^2}\, \mathbf{1} , \tag{87}$$

and the correlation propagators

$$\langle \phi_0(k,\omega)\ \phi_0(-k,-\omega)\rangle_0 = \frac{2\, \overset{o}{\Gamma}\, k^2}{\left| - i\omega + \overset{o}{\Gamma}\, k^2(\overset{o}{\tau} + k^2)\right|^2} , \tag{88}$$

$$\langle \boldsymbol{j}_t(k,\omega) \otimes \boldsymbol{j}_t(-k,-\omega)\rangle_0 = \frac{2\, \overset{o}{\lambda}_t\, k^2}{\left| - i\omega + a_j\, \overset{o}{\lambda}_t\, k^2\right|^2}\, \mathbf{1} . \tag{89}$$

In the extended model additional propagators of order $(\overset{o}{c})^{-1}$ arise, which contribute in the limit $\overset{o}{c}\to\infty$ with vertices of order $\overset{o}{c}$ to the vertex functions, they read

$$\langle\phi_0(k,\omega)\,\tilde{\boldsymbol{j}}_l(-k,-\omega)\rangle_0 = -\frac{\overset{o}{L}_\phi\,\boldsymbol{k}}{i\,\overset{o}{c}\Big(-i\omega+\overset{o}{\Gamma}k^2(\overset{o}{\tau}+k^2)\Big)}\,, \tag{90}$$

$$\langle\boldsymbol{j}_l(k,\omega)\,\tilde{\phi}_0(-k,-\omega)\rangle_0 = -\frac{\overset{o}{L}_\phi\,(\overset{o}{\tau}+k^2)\boldsymbol{k}}{ia_j\,\overset{o}{c}\Big(-i\omega+\overset{o}{\Gamma}k^2(\overset{o}{\tau}+k^2)\Big)}\,, \tag{91}$$

$$\langle q_0(k,\omega)\,\tilde{\phi}(-k,-\omega)\rangle_0 = -\frac{\overset{o}{g}_l\overset{o}{h}_q}{ia_q\,\overset{o}{c}\Big(-i\omega+\overset{o}{\Gamma}k^2(\overset{o}{\tau}+k^2)\Big)}\,, \tag{92}$$

$$\langle q_0(k,\omega)\,\tilde{\boldsymbol{j}}_l(-k,-\omega)\rangle_0 = \frac{\boldsymbol{k}}{ia_q\,\overset{o}{c}\,k^2}\,, \tag{93}$$

$$\langle\boldsymbol{j}_l(k,\omega)\,\tilde{q}_0(-k,-\omega)\rangle_0 = \frac{\boldsymbol{k}}{ia_j\,\overset{o}{c}\,k^2}\,, \tag{94}$$

$$\langle\phi_0(k,\omega)\,q_0(-k,-\omega)\rangle_0 = \frac{2\,\overset{o}{\Gamma}\,k^2\,\overset{o}{g}_l\overset{o}{h}_q}{a_q\,\overset{o}{c}\Big|-i\omega+\overset{o}{\Gamma}k^2(\overset{o}{\tau}+k^2)\Big|^2}\,, \tag{95}$$

$$\langle\phi_0(k,\omega)\,\boldsymbol{j}_l(-k,-\omega)\rangle_0 = -\frac{2\,\overset{o}{L}_\phi\,\boldsymbol{k}\omega}{a_j\,\overset{o}{c}\Big|-i\omega+\overset{o}{\Gamma}k^2(\overset{o}{\tau}+k^2)\Big|^2}\,. \tag{96}$$

The steps presented here followed quite closely the Lagrangian theory developed by Bausch, Janssen and Wagner 1976 [21].

5.4 Renormalization

We are now in the position to perform the calculation of the relevant vertex functions. It turns out that these functions have singularities and within the concept of RG theory these singularities are put into renormalization constants [21].

From the renormalization constants one finds the ζ-functions and these lead to β-functions being zero at fixed points. Let us write

$$\ell\frac{df}{d\ell} = \beta_f(\{f\}) \tag{97}$$

where we consider f as the set of all renormalizing model parameters. This equation can be obtained by different methods. Here we have chosen the field theoretic approach. Another method is Wilson's "shell integration" generalized to dynamics (solving perturbationaly the equation of motion of the shell variables. See [22].) Usually for ℓ going to zero the flow comes to rest (then the left hand side and the right hand side of Eq. 97, the β-function is zero[2]) and the parameters f reach

[2]There may (i) be several regions attracted to different fixed points, each having his region

model	ζ-functions	amplitude functions
A	De Dominicis, Brezin, Zinn-Justin 1975 [24]	
B	trivial	
C	Brezin, De Dominicis 1975 [25] corrected by Folk, Moser 2002 [26]	
E	Dohm 1978 [30]	Dohm 1978 [30], 1979 [31]
F	Dohm 1991 [27] corrected by Folk, Moser 2002 [29]	Dohm 1985 [28]
E'	Dohm, Folk 1983 [32]	
F'	Folk, Moser 2002 [29]	new
G	Folk, Moser unpublished, new	
H	DeDominicis, Peliti 1978 [33] corrected by Adzhemyan et al. 1999 [34]	
H'	1-loop Folk, Moser 1995 [35]	
J		1-loop Dohm 1976 [36]
SSS	DeDominicis 1978 [33]	

Table 1: References to the papers where results of field theoretic dynamical RG calculations are presented. A lot of results had to be corrected. The recognition of general structures of the perturbation theory turned out to be of help checking the results for the ζ-function (especially for model C, F, F' and G). This list of papers replaces specific references within this review to the results of these papers.

some values called fixed point values f^*. The region where this happens is called the asymptotic region. Inserting fixed point values into the ζ-functions leads to the universal values of the critical exponents. The physical expressions calculated from vertex functions are functions of the model parameters and choosing the fixed point values for them lead to universal amplitude ratios.

One sees there is more to calculate than the fixed points. It is already clear that one is also interested in the flow properties of the parameters described by the flow equations given by the β functions. Effective exponent and amplitude ratios can then be calculated and compared with experiment. Beside the renormalization the calculation of the amplitude functions is important. An overview on the status of the field theoretic calculations is given in Tab. 1

of attraction. (ii) These regions might be zero, then the fixed point is called unstable. However the unstable fixed point may first attract the flow but finally repells the flow. This leads to the phenomenon of crossover between different types of critical behavior

6 Renormalization and the dynamical exponent z

An important point in the theoretical calculations is the structure of perturbation theory. It turns out that a reduction of graphical contributions is reached by introducing the T_c-shift and the correlations length (note that the correlation length does not renormalize) within the perturbational expansion. This is already know from statics [23].

6.1 Structure and renormalization

More important for dynamics is to recognize that the OP vertex function can be written as

$$\overset{o}{\Gamma}_{\phi\tilde{\phi}}(\xi,k,\omega) = -i\omega\,\overset{o}{\Omega}_{\phi\tilde{\phi}}(\xi,k,\omega) + \overset{o}{\Gamma}{}^{(st)}_{\phi\phi}(\xi,k)\,\overset{o}{\Gamma}\,k^a\,\overset{o}{\bar{\Gamma}}{}^{(d)}_{\phi\tilde{\phi}}(\xi,k,\omega) \tag{98}$$

In this way a seperation of genuine dynamic and static parts has taken place. The renormalization follows the usual lines where the following Z-factors have to be introduced

$$\overset{o}{\Gamma}_{\phi\tilde{\phi}} = Z_\phi^{-1/2} Z_{\tilde{\phi}}^{-1/2}\Gamma_{\phi\tilde{\phi}} \qquad \overset{o}{\Gamma}{}^{(st)}_{\phi\phi} = Z_\phi^{-1}\Gamma^{(st)}_{\phi\phi} \qquad \overset{o}{\Gamma} = Z_\Gamma\Gamma \tag{99}$$

and

$$\overset{o}{\Omega}_{\phi\tilde{\phi}} = Z_{\Omega_{\phi\tilde{\phi}}}\Omega_{\phi\tilde{\phi}} \qquad \overset{o}{\bar{\Gamma}}{}^{(d)}_{\phi\tilde{\phi}} = Z^{(d)}_{\bar{\Gamma}_{\phi\tilde{\phi}}}\bar{\Gamma}^{(d)}_{\phi\tilde{\phi}} \tag{100}$$

The renormalized vertex function leads to certain relations for the corresponding ζ-functions defined as logarithmic derivatives of the Z-factors.

$$\Gamma_{\phi\tilde{\phi}} = -i\omega Z_\phi^{1/2} Z_{\tilde{\phi}}^{1/2} Z_{\Omega_{\phi\tilde{\phi}}}\Omega_{\phi\tilde{\phi}} + Z_\phi^{1/2} Z_{\tilde{\phi}}^{1/2} Z_\phi^{-1}\Gamma^{(st)}_{\phi\phi} Z_\Gamma \Gamma k^a Z^{(d)}_{\bar{\Gamma}_{\phi\tilde{\phi}}}\bar{\Gamma}^{(d)}_{\phi\tilde{\phi}} \tag{101}$$

since the poles are completely removed in both parts. Taking the ζ-functions at the stable fixed point

$$-\zeta^*_{\Omega_{\phi\tilde{\phi}}} = \frac{1}{2}\zeta^*_\phi + \frac{1}{2}\zeta^*_{\tilde{\phi}} \qquad \zeta^*_\phi - \zeta^*_\Gamma - \zeta^{(d)*}_{\bar{\Gamma}_{\phi\tilde{\phi}}} = \frac{1}{2}\zeta^*_\phi + \frac{1}{2}\zeta^*_{\tilde{\phi}} \tag{102}$$

it follows

$$\zeta^*_\Gamma = -\zeta^{(d)*}_{\bar{\Gamma}_{\phi\tilde{\phi}}} + \frac{1}{2}\zeta^*_\phi - \frac{1}{2}\zeta^*_{\tilde{\phi}} = -\zeta^{(d)*}_{\bar{\Gamma}_{\phi\tilde{\phi}}} + \zeta^*_{\Omega_{\phi\tilde{\phi}}} + \zeta^*_\phi \tag{103}$$

This alows one to express the ζ-function for the OP Onsager coefficient by the ζ-functions of the two dynamical parts $\Omega_{\phi\tilde{\phi}}$ and $\bar{\Gamma}^{(d)}_{\phi\tilde{\phi}}$.

6.2 Calculating the dynamical exponent

The characteristic frequency of the OP susceptibility at T_c is given by a power law and defines the dynamical exponent z

$$\omega_c(T_c, k) = Ak^z \tag{104}$$

On the other hand a characteristic frequency is given by

$$\omega_c = \Gamma(\ell)k^{2+a} \qquad \ell = \xi_0 k \tag{105}$$

and the asymptotic solution of the flow equation for Γ. This is given by

$$\Gamma(\ell) \sim \ell^{\zeta_\Gamma^*} \tag{106}$$

and taking everything together one finds the dynamical exponent given by

$$z_\phi = a + 2 + \zeta_\Gamma^* \tag{107}$$

Inserting for ζ_Γ^* the relation found from the vertex function structure one obtains

$$z_\phi = 2 + a + \zeta_\phi^* + \zeta_{\Omega_{\phi\tilde{\phi}}}^* - \zeta_{\bar{\Gamma}_{\phi\tilde{\phi}}}^{(d)*} \tag{108}$$

For a conserved density coupled to the OP one always has $\zeta_{\Omega_{\alpha\tilde{\alpha}}}^* = 0$ and therefore the corresponding dynamical exponent

$$z_\alpha = 2 + \zeta_\alpha^* - \zeta_{\bar{\Gamma}_{\alpha\tilde{\alpha}}}^{(d)*} \tag{109}$$

where a similar structure as for the OP of the dynamical vertex function holds. Strong dynamical scaling states that $z_\phi = z_\alpha$.

From statics it is already known that

$$\zeta_\phi^* = -\eta \qquad \zeta_\alpha^* = \frac{\alpha}{\nu} \tag{110}$$

6.2.1 Models without mode coupling terms

In the relaxational model ($a = 0$)

$$\zeta_{\bar{\Gamma}_{\phi\tilde{\phi}}}^{(d)*} = 0 \tag{111}$$

as in all following models in this subsection and z is written

$$z_\phi = 2 - c\eta \tag{112}$$

where c is calculated from $\zeta^*_{\Omega_{\phi\tilde{\phi}}}$.

When the OP is conserved as in model B ($a = 2$) also

$$\zeta^*_{\Omega_{\phi\tilde{\phi}}} = 0 \tag{113}$$

showing the absence of a genuine dynamic renormalization and

$$z_\phi = 4 - \eta \tag{114}$$

A more complicated situation is in model C ($a = 0$) where a non conserved OP is coupled in the static functional to a conserved density (energy). Let us assume that the specific heat is diverging and strong scaling holds. For the OP we have

$$\zeta^{(d)*}_{\bar{\Gamma}_{\phi\tilde{\phi}}} = 0 \tag{115}$$

and the fixed point value of time ratio $w = \Gamma/\lambda$ is finite and nonzero according to the assumption

$$0 = \beta_w = w^*(\zeta^*_\phi + \zeta^*_{\Omega_{\phi\tilde{\phi}}} - \zeta^*_\alpha) \qquad - \eta + \zeta^*_{\Omega_{\phi\tilde{\phi}}} = \zeta^*_\alpha \tag{116}$$

The secondary density is conserved and the genuine dynamic ζ-functions are zero as in model B. Thus

$$z_\phi = 2 + \frac{\alpha}{\nu} = z_\alpha \tag{117}$$

There may be another fixed point, the weak scaling fixed point, stable. For this fixed point (weak scaling fixed point) $w^* = 0$ and $z_\phi = 2 - c\eta$ and $z_\alpha = 2 + \alpha/\nu$.

6.2.2 Models with mode coupling terms

Ward identities play an important role in critical dynamics since the symmetry properties on which they base determine the Poisson brackets. Moreover since the structure of the renormalized models has the same structure of the unrenormalized model the poisson brackets can be used to find the renormalization factor Z_g of the mode coupling g_0 (of course the mode couplings have naive dimensions which determine the upper dynamical critical dimension above which the mode couplings are irrelevant).

Ward identities make use of symmetries in dimensional space (translation, rotation etc) or in OP-space (rotation etc). Let us discuss an example from statics and consider rotation of the OP in the OP-space ($n = 2$). The rotation matrix R may be written

$$R = \begin{pmatrix} 1 & -\alpha \\ \alpha & 1 \end{pmatrix} \tag{118}$$

The invarianze of the partition function

$$Z(R\vec{H}) = Z(\vec{H}) \tag{119}$$

leads to the Ward identity (the terms proportional to α should be zero)

$$H_1 \frac{\delta Z}{\delta H_2} - H_2 \frac{\delta Z}{\delta H_1} = 0 \tag{120}$$

Similar relation can be derived for vertex functions via Legendre Transformations. From these equations which holds also for the renormalized quantities relations between the Z-factors (the ζ-functions) can bederived. Just to mention another example is the gauge transformation in supeconductors which leads to an expression of the renormalization of the coupling to the gauge field.

Now coming back to dynamics the important observation for model E, F, G, J is that the second conserved density M (besides the conserved or non conserved OP) is the generator of rotations in OP-space. This is reflected by the Poisson bracket (and the renormalized version) between the OP= ϕ and M

$$\{\phi, M\} = g\phi \qquad M = \phi \quad \text{for model J} \tag{121}$$

This leads to the relation

$$Z_g = Z_M^{1/2} = 1 \qquad \text{and} \quad \text{for model J} \quad Z_g = Z_\phi^{1/2} \tag{122}$$

In the case of model H the Galilean invariance is used to calculate the Poisson bracket and the OP and the mass current, which is the generator of movements. This leads to Z_g=1

Knowing the renormalization of the mode coupling g and its naive dimension (easily seen in comparing terms in the Lagrangian) we find additional relations by the conditions of finite fixed point values for the time ratio w and the mode coupling f.

In model E ($a = 0$, specific heat finite, strong scaling) with $w = \Gamma/\lambda$

$$0 = \beta_w = w^*(\zeta_\phi^* + \zeta_{\Omega_{\phi\tilde{\phi}}}^* - \zeta_{\bar{\Gamma}_{\phi\tilde{\phi}}}^{(d)*} + \zeta_\lambda^{(d)*}) \tag{123}$$

and $f = g/\sqrt{\Gamma\lambda}$

$$0 = \beta_f = \frac{1}{2} f^*(4 - d - \zeta_\phi^* - \zeta_{\Omega_{\phi\tilde{\phi}}}^* + \zeta_{\bar{\Gamma}_{\phi\tilde{\phi}}}^{(d)*} + \zeta_\lambda^{(d)*}) \tag{124}$$

this leads to

$$\zeta_\phi^* + \zeta_{\Omega_{\phi\tilde{\phi}}}^* - \zeta_{\bar{\Gamma}_{\phi\tilde{\phi}}}^{(d)*} = \frac{4-d}{2} \tag{125}$$

and to

$$z_\phi = \frac{d}{2} \tag{126}$$

in spatial dimension d. The same value of the dynamical critical exponent may be derived in model G.

In model H ($a = 2$) the OP and the secondary density scale differently, both are densities of conserved quantities. Defining the mode coupling as $f = g/\sqrt{\Gamma\lambda_t}$ from its finite fixed point value follows

$$0 = \beta_f = \frac{1}{2} f^* (4 - d + \zeta_\phi^* + \zeta_{\bar{\Gamma}_{\phi\tilde{\phi}}}^{(d)*} + \zeta_{\lambda_t}^{(d)*}) \tag{127}$$

This leads to a relation between the two dynamical exponents - for the two kinetic coefficients, shear viscosity and thermal conductivity In $d = 3$ it reads

$$\zeta_{\Gamma_{\phi\tilde{\phi}}}^{(d)*} + \zeta_{\lambda_t}^{(d)*} = 1 - \eta \tag{128}$$

Thus z has to be calculated explicitely from one dynamic ζ-function.

In Model J ($a = 2$, OP conserved) the finite fixed point value of the mode coupling $f = g/\Gamma$ leads to

$$0 = \beta_f = f^* \left(\frac{6 - d}{2} + \frac{1}{2}\zeta_\phi^* - \zeta_{\bar{\Gamma}_{\phi\tilde{\phi}}}^{(d)*} \right) \tag{129}$$

and

$$\zeta_\phi^* + \zeta_{\Omega_{\phi\tilde{\phi}}}^* - \zeta_{\bar{\Gamma}_{\phi\tilde{\phi}}}^{(d)*} = -\frac{6 - d}{2} - \zeta_\phi^* \tag{130}$$

and the dynamic critical exponent

$$z_\phi = \frac{2 + d - \eta}{2} \tag{131}$$

Note that in all cases the naive dimension of the mode coupling g is $(4-d)/2$ except model J where it is $(6-d)/2$. Thus the static upper borderline dimension for the irrevelance of the static coupling u is different from that for the irrelevance of the mode coupling g in model J.

7 Comparison with experiment

7.1 General procedure

Since we are not only interested in the asymptotic region where the coupling parameters of the model (static and dynamic) as well as the time scale ratios take on

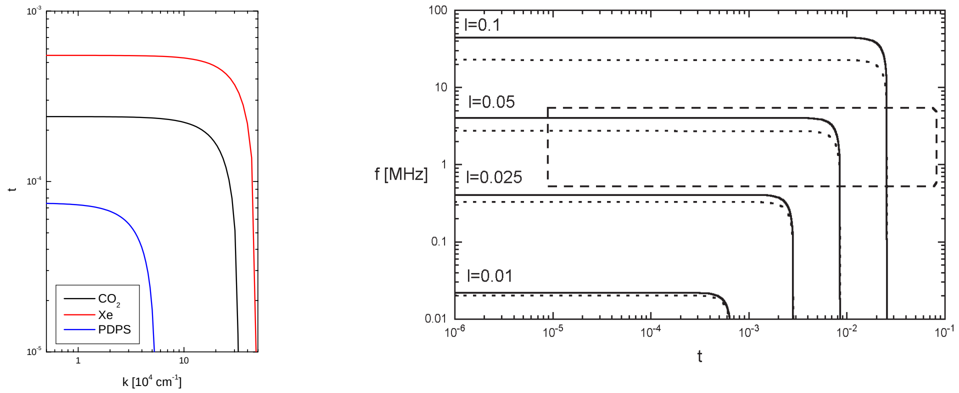

Figure 7: (a) Comparison of the matching condition at zero frequency for different fluids and (b) comparison at zero wave vector of asymptotic matching lines (dotted curves) with non-asymptotic lines in one fluid. The dashed frame gives the region where sound experiments are made.

their fixed point values the comparison with experiment involves the flow equations describing the change of the model parameters mentioned. The general form of these equations are e.g. for the fluid without coupling to the sound mode (model H in one loop order)

$$\ell \frac{d\Gamma}{d\ell} = -\frac{3}{4}\Gamma f_t^2 \tag{132}$$

$$\ell \frac{df_t}{d\ell} = -\frac{1}{2} f_t (1 - \frac{19}{24} f_t^2) \tag{133}$$

In order to get the dependence of the parameters on the physical quantities as the relative temperature distance from the phase transition temperature (or on the correlation length), the wave vector and the frequency we have to connect the arbitrary flow parameter ℓ to these variables. This is achieved by formulating a suitable matching condition usually found by the condition that certain logarithmic terms in the calculated vertex functions are zero. This also guarantees that the vertex functions are finite in all the limits one may consider. E.g. for fluids one has for the cases where one calculates vertex functions at zero frequency or zero wave vector (see Fig. 7)

$$\ell^2 = \left(\frac{\xi_0}{\xi(t)}\right)^2 + (\xi_0 k)^2 \qquad \text{or} \tag{134}$$

$$\ell^8 = \left(\frac{\xi_0}{\xi(t,\Delta\rho)}\right)^8 + \left(\frac{2\omega}{\Gamma(\ell)}\right)^2 \tag{135}$$

respectively. Note that the matching condition contains non universal parameters like ξ_0 or remain implicite equations for ℓ as in the second case and need the solution of the flow equations.

7.2 Fluids: The linewidth in light scattering

7.2.1 Theoretical result in one loop order

Calculating the dynamic susceptibility in one loop order leads to a Lorentzian shape function (this is not quite understood, since one would expect a one loop correction which is absent)

$$\chi_{dyn}(k,\xi,\omega) = \frac{\chi_{st}(k,\xi)}{\omega_c(k,\xi)} \frac{2}{1+y^2} \qquad y = \omega/\omega_c \tag{136}$$

and a half width at half heigth

$$\omega_c(k,\xi) = \Gamma(\ell)\, k^2(\xi^{-2}+k^2) \left\{ 1 - \frac{f_t^2(\ell)}{16} \left[-5 + 6\,(k\xi)^{-2} \ln(1+(k\xi)^2) \right] \right\} \tag{137}$$

The flow parameter ℓ has to be replaced by the matching condition and the functions of the mode coupling $f(\ell)$ and $\Gamma(\ell)$ have to replaced by the solutions of the corresponding flow equations. This can be done analytically in one loop order to give

$$\omega_c(k,x) = \Gamma_{as}\, k^z \left(\frac{1+x^2}{x^2} \right)^{1-x_\lambda/2} c_{na}(k,x)^{x_\lambda} f(k,x) \tag{138}$$

$$c_{na}(k,x) = \left[1 + \frac{k}{k_0} \sqrt{\frac{1+x^2}{x^2}} \right] \qquad f^* = \sqrt{\frac{24}{19}} \qquad x_\lambda = \frac{18}{19} \tag{139}$$

$$f(k,x) = 1 - \frac{f^{*2}}{16\, c_{na}(k,x)} \left[-5 + 6\, x^{-2} \ln(1+x^2) \right] \tag{140}$$

$$x = k\xi(t) \qquad \Gamma_{as} = \Gamma_0 \left(\frac{19}{24} \frac{f_0^2 \ell_0}{\xi_0} \right)^{x_\lambda} \qquad k_0^{-1} = \left(\frac{24}{19 f_0^2} - 1 \right) \frac{\xi_0}{\ell_0} \tag{141}$$

We are now in the position to discuss all the different limits of this expression: the asymptotic, the non-asymptotic limit and within these limits the crossover from the hydrodynamic to the critical region.

7.2.2 Limiting behavior

Depending on the region in the ξ^{-1}-k-plane (see Fig. 5) where one performs an experiment one may simplify the expression for the characteristic frequency.

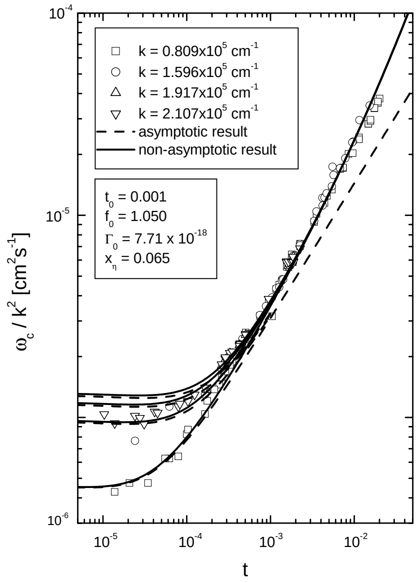

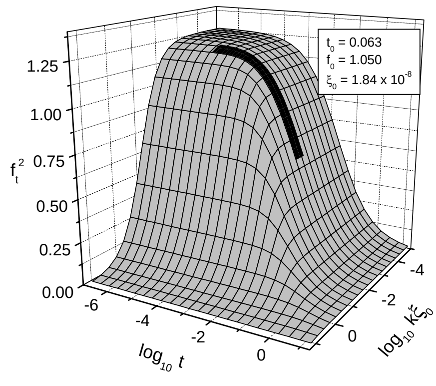

Figure 8: (a) Asymptotic (dashed) and non asymptotic expressions (full) calculated in ε-expansion. f_0 is parameter, Γ_0 taken from the shear viscosity. (b) 'Mountain' of mode coupling f. The black region is the experimental region and it is seen that f is differnt from the fixed point value (the plateau) in most of the region.

In the asymptotic region the mode coupling asumes its fixed point value thus $f_0 \to f^* = \sqrt{24/19}$ that means $k_0 \to \infty$. Thus starting from the beginning with the fixed point value we have

$$\omega_c(k,x) = \Gamma_0\, k^4 (k\xi_0/\ell_0)^{-x_\lambda} \left(\frac{1+x^2}{x^2}\right)^{1-x_\lambda/2} f(k,x) \tag{142}$$

with

$$f(k,x) = 1 - \frac{f^{*2}}{16}\left[-5 + 6\,x^{-2}\,\ln(1+x^2)\right] \tag{143}$$

In the 'opposite' (background) limit the mode coupling goes to zero $f_0 \to 0$ that means $k_0 \to 0$ and $f(k,x) \to 1$ and the Van Hove scaling function is recovered

$$\omega_c(k,x) = \Gamma_0\, k^4 \left(\frac{1}{x^2} + 1\right) \tag{144}$$

In the hydrodynamic limit (asymptotic or non asymptotic) ($k\xi \to 0$) the characteristic frequency depends quadratic on the wave vector

$$\omega_c(k,\xi) = \Gamma_{as}\, k^2\, \xi^{-2+x_\lambda} \left[1+\frac{1}{\xi k_0}\right]^{x_\lambda} \left\{1-\frac{f^{*2}}{16}\left[1+\frac{1}{\xi k_0}\right]^{-1}\right\} \tag{145}$$

the temperature dependence shows the crossover from the Van Hove behavior $D \sim \xi^{-2}$ to the asymptotic behavior $D \sim \xi^{-2+x_\lambda}$.

In the critical limit ($k\xi \to \infty$, $z = 4 - x_\lambda$) we find

$$\omega_c(k) = \Gamma_{as}\, k^z \left[1+\frac{k}{k_0}\right]^{x_\lambda} \left\{1+\frac{5f^{*2}}{16}\left[1+\frac{k}{k_0}\right]^{-1}\right\} \tag{146}$$

Again a crossover from the asymptotic regime ($D \sim k^z$) to the van Hove regime ($D \sim k^4$) at larger values of k takes place.

In Fig. 8a we compare our result with experiments in Xenon. The crossover from the non asymptotic regime (solid curve) to the asymptotic regime (dashed curves asymptotic result $f_0 = f^*$) is seen. This is more explicite shown in Fig. 8b where we have plotted the value of the mode coupling as function of wave vector and temperature. The black region is the region of the experiments. The plot is obtained from the solution of the flow equations with the initial conditions found in the comparison with the experiment in Xe, using the matching condition and for the correlation length $\xi = \xi_0 t^{-\nu}$.

7.2.3 Remarks on the shear viscosity

A similar analysis at $k = 0$ but $\omega \neq 0$ has been performed for the shear viscosity leading to the solid curves in Fig. 1. The experiments on earth take into account gravity and demonstrate for Xe (Fig. 1a) that the effect of frequency dependence is superimposed by the gravity effect. It should however be noted that agreement with the frequency dependence in microgravitiy can only be reached by adjusting the frequency scale by a parameter $A \neq 1$. This parameter is introduced to simulate the effects of two loop order terms. Such a two loop calculation has not been done so far. The density dependence which is used in the calculation of gravity effects is well represented by the results of RG theory (Fig. 1b).

7.3 Ferromagnets: The shape function

The complete scattering function in the asymptotic region for the ferromagnet in one loop order has been calculated but with another method than field theory [37]. The expression allows to discuss the already mentioned shape crossover between the hydrodynamic and critical region. The comparison at T_c demonstrates agreement with the critical shape (see the solid lines in Fig. 3). This shape may be approximated by (such a form has been suggested earlier in [38]

$$F(y, \infty) = \Re \frac{1}{iy + (a + iby)^{\frac{z-4}{z}}} \tag{147}$$

where the parameters $a = 1.51$ and $b = 0.89$ are determined by RG theory.

The peak position in the constant energy scans depend on the shape and the change in this position when crossing over from the critical to the hydrodynamic regime. Satisfactory agreement in Ni [39] has been reached by changing the parameters in the complete result [37]. The decay of the shape function was also measured (in a region 100 times large than the half width) and a decay exponent of 2.3 (prediction of RG 2.6) was found.

The comparison of predictions of RG theory is complicated by the fact that besides the Heisenberg interaction in most cases also dipolar forces are present. This complicates the analysis since the dipolar critical behavior is the asymptotic behavior and one may observe crossover behavior. This makes important computer simulations which simulate 'ideal' Heisenberg ferromagnets, however other problems arise like finite size scaling and time problems due to critical slowing down. Nevertheless for some aspects agreement with RG theory has been found in [40].

7.4 Superfluid Transition: The thermal conductivity

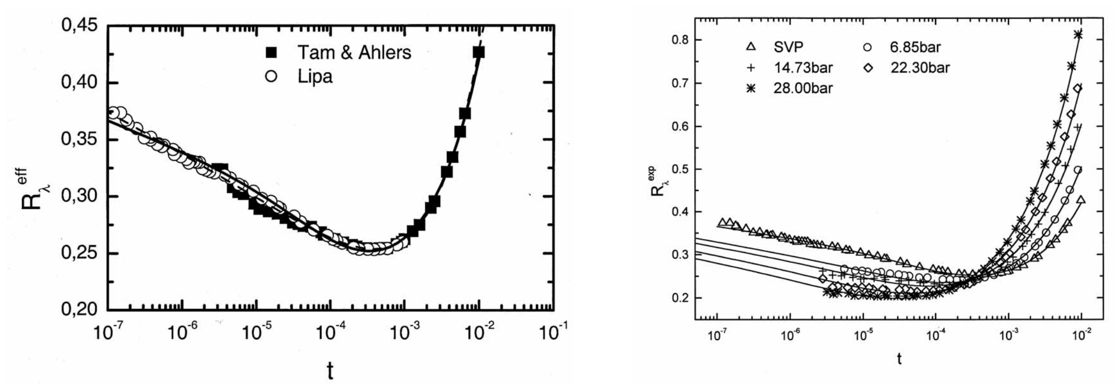

Figure 9: (a) Amplitude ratio for the themal conductivity in ^{4}He at saturated vapor pressure and (b) higher pressures and fits with theory containing dynamical background values as parameters

Within model F one needs for a comparison with experiment the theoretical expression for the amplitude function of the thermal conductivity and the flow equations for the coupling parameters of the model. The most difficult quantity to calculate is the ζ-function of the OP kinetic coefficient Γ. This has been achieved recently

$$\zeta_\Gamma = \mathcal{F}^2 + \frac{u^2}{9}\left(L_0 + x_1 L_1 - \frac{1}{2}\right) - \frac{2}{3}u\mathcal{F}a - \frac{1}{2}\mathcal{F}^2 b \tag{148}$$

$$\zeta_\lambda = \gamma^2 - \frac{F^2}{2w'}\Big(1 + \frac{1}{2}\Re[Q]\Big) \tag{149}$$

where $\mathcal{F} = \mathcal{C} - i\mathcal{E}$, $\mathcal{C} = \sqrt{\frac{w}{1+w}}\ \gamma$, $\mathcal{E} = \frac{F}{\sqrt{w(1+w)}}$, $\Gamma = \Gamma' + i\Gamma''$, $w = \Gamma/\lambda$, $F = g/\lambda$, $f = F^2/w'$ and the other quantities not mentioned are functions of F and w. With this result we have reanalyzed the effective amplitude (M are the toop loop contributions).

$$R_\lambda^{eff} = \frac{1 - f/4 + fM(w, F, \gamma, u)}{2\sqrt{\pi f w'(1 + \gamma^2 F_+(u))}} \tag{150}$$

Parameters in the fits of the effective amplitude (see Fig. 9) are the background values of f and w. The main result of the correction of the earlier result for ζ_Γ is the background value found for the imaginary part w''. This value was predicted [41] to be (unrenormalized) $w_0'' = 0.21$ at SVP and the renormalized background value found is $w'' = 0.3$ instead of $w'' = 0.8$ found earlier [27].

The reason for the dominance of the non asymptotic behavior lies in the circumstance that the dynamical fixed point (w^*, f^*) lies near a stability border line where the scaling fixed point ($w'* \neq 0$, $w''^* = 0$, $f^* \neq 0$, $z_\phi = z_\alpha$) changes stability with the non scaling fixed point ($w'^* = 0$, $w''^* = 0$, $f^* \neq 0$ $z_\phi \neq z_\alpha$) *and* w' appears in the denominator of R_λ^{eff}. Near a stability border line the at least one transient exponent goes to zero and the value of $w'* \sim 0$. It turns out that it depends on the fixed point value u^* which of the dynamic fixed points is stable, but this is only of little relevanz in the physical accessible region.

Acknowlegement: I want to thank G. Moser for cooperation in this field. The progress made in the last years is based on work done with him. I also thank all other authors with whome I worked together in this field. They all stimulated me to stay within the field of critical dynamics. I also want to thank Maxym Dudka for reading the manuscript and helpful comments. Work supported by FWF project P15247.

References

[1] D. J. Amit, *Field Theory, the Renormalization Group, and Critical Phenomena*, McGraw Hill London 1978
J.J. Binney et al, *The Theory of Critical Phenomena. An Introduction to the*

Renomalization Group, Clarendon Press Oxford 1992
H. Kleinert and Verena Schulte Frohlinde, *Critical Properties of* Φ^4*-Theory*, World Scientific Singapore 2001

[2] P.C.Hohenberg and B.I.Halperin, Rev.Mod.Phys. **49**, 435 (1977)

[3] R. F. Berg, M. R. Moldover, and G. A. Zimmerli, Phys. Rev. Lett. **82**, 920 (1999); Phys. Rev. E **60**, 4079 (1999)

[4] R. F. Berg and M. R. Moldover, J. Chem. Phys. **93**, 1926 (1990)

[5] H. Iwasaki and M. Takahashi, J. Chem. Phys. **74**, 1930 (1981)

[6] Jan V. Sengers, in Ed. Kiran and J. M. H. Levelt Sengers *Supercritical fluids* Kluwer Academic Publishers pages 231-271 (1994)

[7] P. Böni, M. E. Chem, and G. Shirane, Phys. Rev. B **35**, 8449 (1987)

[8] W. Y. Tam and G. Ahlers, Phys. Rev. B **33**, 133 (1986)

[9] Q. Li, PhD Thesis, Stanford University (1991); J. A. Lipa and Q. Li, Czech. J. Phys. **46**, 185 (1996)

[10] Phys. Rev. **93**, 268 (1954); **95**, 249 (1954); **95**, 1374 (1954)

[11] R. A. Ferrell, N. Menyhard, H. Schmidt, F. Schwabl, and P. Szepfalusy, Phys. Rev. Lett. **18**, 891; Phys. Lett. **24A**, 493

[12] H. L. Swinney and D. L. Henry, Phys. Rev. A **8**, 2586 (1973)

[13] R. Folk and G. Moser **57**, 683 (1998)

[14] A.Onuki, J.Low Temp.Phys. **53**, 1 (1983)

[15] M.S.Green, J.Chem.Phys. **20**, 1281 (1952)

[16] R.W.Zwanzig, J.Chem.Phys. **33**, 1338 (1960), Phys.Rev. **124**, 983 (1961)

[17] H.Mori, H.Fujisaka, Prog.Theor.Phys. **49**, 764 (1973)

[18] H.Mori, H.Fujisaka, H.Shigematsu, Prog.Theor.Phys. **51**, 109 (1974)

[19] K.Kawasaki, 'Phase Transitions and Critical Phenomena', Vol.5a, ed. C.Domb and M.S.Green, Academic Press (1975)

[20] I.E. Dzyaloshinskii, G.E.Volovick, Ann.Phys.(N.Y.) **125**, 67 (1980)

[21] R.Bausch, H.K.Janssen, H.Wagner, Z.Phys.B **24**, 113 (1976)

[22] Shang-Keng Ma, *Modern Theory of Critical Phenomena*, Benjamin 1976

[23] R.Schloms and V.Dohm, Nucl.Phys.B **328** (1989)

[24] C. De Dominicis, E. Brezin and J. Zinn-Justin, Phys. Rev. B **12**, 4945 (1975) (model A)

[25] E. Brezin and C. De Dominicis, Phys. Rev. B **12**, 4954 (1975) (model C)

[26] R. Folk and G. Moser, acta physica slovaca **52**, 285 (2002) and submitted to Phys. Rev. Lett. (2003)

[27] V. Dohm, Phys. Rev. B **44**, 2697 (1991) (model F) ζ-functions)

[28] V. Dohm, Z. Phys. B **61**, 193 (1985) (amplitude function for the thermal conductivity)

[29] R. Folk and G. Moser, Phys. Rev. Lett. **89**, 125301 (2002)

[30] V. Dohm, Z. Phys. B **31**, 327 (1978)

[31] V. Dohm, Z. Phys. B **33**, 79 (1979)

[32] V. Dohm, R. Folk, Phys. Rev. B **28**, 1332 (1983)

[33] C. De Dominicis and L. Peliti, Phys. Rev. B **18**, 353 (1978) (model H)

[34] L. Ts. Adzhemyan et al., Theoret. Math. Phys. **119**, 454 (1999) (model H)

[35] R. Folk and G. Moser, Phys. Rev. Lett. **75**, 2706 (1995) and Phys. Rev. E **58**, 6246 (1998) (model H')

[36] V. Dohm, Solid State Comm. **20**, 657 (1976)

[37] H. Iro, Z. Phys. B **68**, 485 (1987); Journal de Physique, **49** C8 - 1563 (1988); J. Magn. Mat Mater. **73**, 175 (1988)

[38] K. Bhattacharjee and R. A. Ferrell, Phys. Rev. B **24**, 6480 (1981)

[39] P. Böni, H. A. Mook, J. L. Martinez and G. Shirane, Phys. Rev. B **47**, 3171 (1993)

[40] Kun Chen and D. P. Landau, Phys. Rev. B **49**, 3266 (1994)

[41] V. Dohm, Phys. Rev. B **29**, 1497 (1984)